1-2017

Freeze-thaw Durability of Concrete Columns Wrapped with FRP and Subject to Corrosion-Like Expansion

Ronald S. Harichandran
University of New Haven, rharichandran@newhaven.edu

M.I. Baiyasi
Elsinore Valley Municipal Water District

G. Nossoni
Manhattan College

Publisher Citation

Harichandran, R. S., Baiyasi, M. I., and Nossoni, G. (2016). "Freeze-thaw durability of concrete columns wrapped with FRP and subject to corrosion-like expansion." Journal of Materials in Civil Engineering, 29(1).

Comments

This is the authors' accepted manuscript of the article published in *Journal of Materials in Civil Engineering*. The version of record can be found at http://dx.doi.org/10.1061/(ASCE)MT.1943-5533.0001691#sthash.JA9OUibt.dpuf

FREEZE-THAW DURABILITY OF CONCRETE COLUMNS WRAPPED WITH FRP AND SUBJECT TO CORROSION-LIKE EXPANSION

R. S. Harichandran,[1] M. I. Baiyasi[2] and G. Nossoni[3]

ABSTRACT

Experiments were conducted to assess the effects of using fiber-reinforced polymer (FRP) wraps, with fibers oriented in the hoop direction, for rehabilitating corrosion-damaged columns. This paper reports findings related to the freeze-thaw durability of concrete specimens with round and square cross sections, wrapped with glass and carbon FRP, after they are subjected to an internal expansive force similar to that generated by corroding steel. The results of the experiment indicate that freeze-thaw cycles have no statistically significant effect on the compressive strength of glass and carbon wrapped specimens. Freeze-thaw conditioning generally reduced the longitudinal failure strain of wrapped specimens. The square wrapped specimens had lower compressive strength compared to the round specimens, even though the cross sectional area of the square prisms was higher than that of the round cylinders. This is due to the reduced confinement provided by the wraps for square cross sections and stress concentrations that develop at the corners. Wrapped square prisms always failed by rupture of the wrap at a corner. A reduction of approximately 30% to 40%

[1] Dean, Tagliatela College of Engineering, University of New Haven, West Haven, CT 06516.
[2] Manager, Elsinore Valley Municipal Water District, 31315 Chaney St, Lake Elsinore, CA 92530
[3] Asst. Prof., Department of Civil and Environmental Engineering, Manhattan College, Riverdale, NY 10471.

in failure stress was noted between wrapped specimens with round and square cross sections, respectively.

INTRODUCTION

One of the main causes of deterioration in reinforced concrete structures is corrosion of the reinforcement bars (Du et al. 2006). The strength, durability and service life of concrete structures are reduced by corrosion. Corrosion products can have a volume of up to 600% of the original volume of the corroding steel (Mehta and Monteiro 1993). This extra volume applies pressure to the surrounding concrete and causes cracking and delamination of the concrete cover. Both oxygen and chloride is required for the corrosion activity to start. If a barrier reduces the diffusion of oxygen and chloride into concrete, then the time to corrosion will reduce considerably. Using FRP wraps is one way to introduce a barrier that retards the diffusion of oxygen and chloride into concrete, thereby increasing the service life and durability of concrete structures (Nossoni 2015).

FRP materials have been used over the past two decades in civil engineering structures for different strengthening applications because of their superior mechanical properties as well as their resistance to aggressive environmental conditions. However, some environmental factors such as extreme temperature fluctuation and water absorption can adversely affect the behavior of some polymer composite material. Water absorption reduces the strength and stiffness of some polymeric composites by as much as 30% compared to dry material. Water absorption can break down the interface between the reinforcing fiber and resin matrix leading to loss of strength and rigidity. Cycles of freezing and thawing tend to magnify the effect of water absorption (Gomez and Casto 1996).

While several studies have been conducted on the strength of columns wrapped with FRPs, studies on durability under harsh environmental conditions such as freeze-thaw and exposure to chloride are much fewer (Soudki 1997, Toutanji and Balaguru 1998, Rivera and Karbhari 1999, Almusallam et al. 2000, El-Zefzafy et al. 2011). Also, most of these studies focused on the deterioration of the FRP and concrete bond rather than the behavior of the FRP wrap under these harsh environments (Karbhari and Zhao 1998, Colombi et al. 2009, Shi et al. 2013, Silva and Bicaia 2008, Yun and Wu 2011). Results from most studies indicated that freeze-thaw cycling does not have a significant effect on the bond strength between FRP and concrete and most of the specimens failed in the concrete substrate and not along the bonded surface (Chajes et al. 1994, Colombi et al. 2009, Silva and Biscaia 2008, Toutanji and El-Korchi 1999, Karbhari and Zhao 1998). However, one study found that the failure was more brittle after freeze-thaw cycling (Karbhari and Zhao 1998).

A few studies reported the effect of harsh environment on FRP strength and the final confined concrete strength of FRP-wrapped concrete specimens after exposure. Specimens wrapped with CFRP experienced no reduction in strength or ductility due to wet-dry exposure, whereas specimens wrapped with GFRP experienced more reduction in both strength and ductility (Li and Karbhari 2003, Rivera and Karbhari and Zhao 1998, Toutanji and Balaguru 1998, Steckel et al. 1998, Nardone et al. 2012). However, a study by Chin et al. (1997) concluded that there was no significant reduction in the tensile strength of GFRP when it was exposed to salt and distilled water for more than 1300 hours.

In a few studies the durability and strength of FRP-wrapped concrete columns under simultaneous loading and environmental exposure was reported. Green et al. (2006) studied the effect of sustained load and freeze-thaw cycles at the same time and concluded that

confined concrete strength was not reduced significantly for normal strength concrete. However, there appears to be no research that investigated the simultaneous effect of freeze-thaw cycling and corrosion of reinforcing bars. Usually corrosion of steel bars occurs due to deicing salts, and the corrosion of steel bars and freeze thaw cycles can occur simultaneously.

In the research reported herein, a comprehensive experimental study was performed to investigate the strength of FRP-wrapped cylinders when they were subjected to a sequence of different environmental exposure conditions. First, the cylinders were subjected to corrosion-like expansion and then to freeze-thaw conditioning. Corrosion-induced expansion was simulated using the expanding cement Bristar. The expansion due to Bristar was calibrated using experiments and validated using an analytical solution and finite element analysis. Subsequently, the samples were subjected to 300 freeze-thaw cycles to study the effect of both conditions on the compressive strength of the confined concrete.

EXPERIMENTAL WORK

Durability of FRP Panel

First the effect of freeze-thaw and wet-dry cycles on the durability of two different types of FRP, glass FRP (GFRP) and carbon FRP (CFRP), was investigated. Four-ply GFRP and two-ply CFRP sheets were fabricated using the wet lay-up process. The samples were cured in air for 5 days according to vender recommendations. After curing, the FRP panels were subjected to 300 freeze-thaw cycles. Subsequently, the FRP panels were cut into coupons and strain gauges were mounted on the coupons. The width of the test specimens varied from 13 to 19 mm (0.5 to 0.75 in.) and their length varied from 190 to 230 mm (7.5 to 9.0 in.), depending on the test. The gage length over which strains were measured was 89 mm (3.5 in.). The test machine was equipped with hydraulically actuated wedge grips

with serrated faces. The FRP coupons were tested under tension to determine the tensile strength, f_u, ultimate strain, ε_u, and elastic modulus, E, of both the conditioned and unconditioned sheets. All the tested coupons were selected from one GFRP panel and one CFRP panel.

Durability of Confined Concrete

Sample preparation: After evaluation of the FRP panels, the effect of simultaneous corrosion-like expansion and freeze-thaw cycles on the durability and strength of FRP-wrapped concrete specimens was investigated. Ready mixed concrete with a water/cement (w/c) ratio of 0.4 and an air entraining admixture was used. The 28-day mean compressive strength of the concrete was 37.7 MPa (5,468 psi). A total of 30 specimens were cast. Two different types of specimens were used; round cylinders with a diameter of 152 mm (6 in.) and a height of 305 mm (12 in.), and square prisms with a 152 mm × 152 mm cross section and a 305 mm height. The corners of the square prisms were rounded to a 13 mm (0.5 in.) radius. Since natural or accelerated corrosion tests are time consuming, an expanding cement known as Bristar was used to simulate the expansion due to corrosion of reinforcing bars. Out of 30 specimens, 24 specimens (12 round and 12 square), were fabricated with a 38 mm (1.5 in.) diameter center hole in the longitudinal direction, and 6 specimens were cast as solid round cylinders. The six solid round specimens without a center hole were not wrapped and kept as control specimens. Solid square specimens without a center hole were not cast because the strength of unwrapped concrete samples is not affected significantly by the geometry of the cross section. The specimens with a center hole were wrapped with FRP and then the center hole was filled with Bristar. The expansion force exerted by Bristar could be controlled with the water to Bristar ratio and was calibrated using experiments, and analytical

and finite element modeling. Although steel rebars were not used, chloride was introduced into the concrete by mixing 11 kg of $NaCl/m^3$ of concrete, which translates to 2% Cl^- ions by weight of cement (Arya and Said-Shawaqi 1996) during casting in order to simulate contaminated concrete.

Wrapping: After 28 days of curing, out of a total of 24 wrapped specimens, 12 were wrapped with three layers of GFRP and 12 with two layers of CFRP having fibers orientated in the hoop direction. All wrapped specimens were subjected to expansion using Bristar one week after wrapping.

Freeze-Thaw: After the initial expansion period of Bristar, which was about one week, 15 specimens (12 wrapped and 3 unwrapped) were exposed to 300 freeze-thaw cycles according to the ASTM C666 procedure and the other 15 samples were kept as control specimens. Table 1 shows the number of samples in each batch.

Strain Gauge Placement: Strain gauges were used to monitor wrap hoop strains during Bristar-induced expansion, and freeze-thaw and compression tests. Six round specimens and six square specimens (three for each type of wrap) that were to undergo 300 cycles of freeze-thaw and four control specimen (one for each type of wrap and specimen shape) were fitted with strain gauges. Each specimen was fitted with two strain gauges oriented in the circumferential direction and placed opposite each other at mid-height. The gauges were coated with wax and silicon to provide moisture and mechanical protection.

Bristar: The effectiveness of using Bristar to simulate corrosion-induced expansion was initially tested on some trial specimens. The expansive nature of Bristar caused the trial specimens to expand in the hoop direction as desired. However, an undesirable side effect was the simultaneous expansion in the longitudinal direction. This caused the trial specimens

with the carbon wrap to split across a cross sectional plane since the carbon wrap contained no longitudinal fibers. The glass wrap had bidirectional fibers and the fibers in the longitudinal direction prevented the specimens from splitting. Additional longitudinal reinforcement was provided to the carbon-wrapped test specimens by strengthening with 51 mm (2 in.) wide strips of carbon in the longitudinal direction. The strips were spaced with 51 mm (2 in.) gaps between them around the circumference. The strain gauge readings were not affected because the strips were placed adjacent to the gauges and the longitudinal strips did not provide any additional lateral confinement.

BRISTAR CALIBRATION

The Bristar mix was used to simulate the internal pressure applied by corroding reinforcing bars. The amount Bistar expands is highly dependent on the water to Bristar ratio. An attempt was made to calibrate the water/Bristar ratio so that a confining pressure in the FRP wraps similar to that developed by corrosion-induced expansion could be generated. Experimental testing was initially performed and then analytical calculations were conducted to calibrate the internal pressure of Bristar expansion to match the pressure due to corrosion of steel bars resulting from a 33% mass loss reported by Harichandran and Baiyasi (2000). Later, the results were validated using finite element simulations.

Experimental Testing

Two concrete specimens to be used for calibration were cast in 4.77 mm thick steel tubes having the same dimensions of a 152 mm diameter, 305 mm height, and a 38 mm center hole. Strain gauges were mounted on the steel tube to monitor its hoop strain. After the concrete was allowed to cure for 28 days, Bristar was prepared with the two different water/Bristar ratios of 0.4 and 0.5 and was poured into the center hole. The strains developed

160 in the steel tubes were monitored for 9-13 days until Bristar reached its final volume and the
161 strains stabilized. Figure 1 shows the strain developed in the steel tube in the calibration
162 samples. The strain in the steel tube reached 380 microstrains (με) in about 4 days for the
163 water/Bristar ratio of 0.5 and around 660 με in about 7 days for the water/Bristar ratio of 0.4.

164 **Analytical Method**

165 From the mechanics of thin walled cylinders, the confining pressure in a confined
166 column is given by

167 $$f_r = \frac{2(E\ \varepsilon_t t n)}{D} \quad (1)$$

168 where t = thickness of the steel tube or wrap per layer, ε_t = circumferential strain of the tube,
169 E = elastic modulus of the tube, n = number of FRP or steel tube layers and D = diameter of
170 the cylindrical column.

171 Using Equation 1, the confining pressures in the steel tube were estimated from the
172 maximum hoop strain in the steel tube shown in Figure 1 for the two different water/Bristar
173 ratios. The maximum confining pressures calculated using Equation 1 were 4.76 MPa
174 (690 psi) and 8.27 MPa (1200 psi) for water/Bristar ratios of 0.5 and 0.4, respectively, and
175 are shown in Table 2. Assuming that the same confining pressures would be developed if
176 three layers of GFRP wrap confined the specimens instead of the steel tube, the hoop strains
177 in the GFRP wrap were back calculated using Equation 1. The hoop strain in a 3-layer GFRP
178 wrap that would induce the confining pressures of 4.76 and 8.27 MPa were estimated to be
179 4,500 με and 7,800 με, respectively. These hoop strains were compared with those in a 3-
180 layer GFRP wrap reported by Harichandran and Baiyasi (2000) for a 33% mass loss resulting
181 from accelerated corrosion for 190 days. Harichandran and Baiyasi studied the effect of

182 bonded and unbonded FRP wraps on the corrosion rate and used 152 mm diameter and
183 305 mm high concrete cylindrical specimens (the same as the calibration specimens in this
184 study), with four #13 steel reinforcing bars placed with 13 mm of cover. They used two bars
185 as anodes and two bars as cathodes to keep the corrosion products within the specimens as in
186 natural corrosion. Figure 2 shows the GFRP strains reported by Harichandran and Baiyasi
187 (2000) for one specimen. The strain gauge was located at the crack location and yielded a
188 strain of about 4,000 με. Comparing this strain with the GFRP wrap hoop strains of 4,500 με
189 and 7,800 με for the water/Bristar ratios of 0.4 and 0.5, respectively, calculated from
190 Equation 1, the water/Bristar ratio of 0.5 appeared appropriate for the experimental study.

191 **Numerical Validation**

192 The analytical model assumes that the expanding Bristar causes the same confining
193 pressure to be applied by the steel tube and GFRP wrap. This assumption is inaccurate
194 because the stiffness of steel and GFRP is different. The GFRP wrap will expand more than
195 the steel tube resulting in a lower confining pressure. A finite element model can capture this
196 behavior and was used to verify whether the water/Bristar ratio of 0.5 was indeed appropriate
197 for the experimental study.

198 The general-purpose FE program ABAQUS (Version 6.12) was used. First, an FE
199 model of the calibration specimen with the steel tube and the center hole was analyzed. In the
200 FE analysis, a uniform radial pressure was applied to the inside surfaces of the center hole of
201 the round calibration specimens to simulate the pressure exerted by expanding Bristar. Since
202 the round calibration specimens were radially symmetric, only one quarter of the specimens
203 was modeled in the FE analysis and appropriate boundary conditions were applied (i.e., free
204 movement of boundary nodes in the radial and longitudinal directions). The insets in Figures

205 3 and 4 show the finite element meshes used. The material models used in ABAQUS are
206 described below.

207 *Concrete:* The Drucker-Prager plasticity model in ABAQUS was used to model the
208 behavior of the confined concrete. The main parameters of the model, such as dilation and
209 friction angles, were selected from the literature (Yu et al, 2010). Other parameters of the
210 model included the concrete compressive strength and elastic modulus, which were obtained
211 through laboratory testing and the ACI equation (i.e., $E_C = 4700\sqrt{f'_c}$ MPa), respectively,
212 and are listed in Table 3.

213 *Steel Reinforcement:* The steel tube in the calibration specimen was modeled as an
214 isotropic elastic-perfectly plastic material. The parameters required for the material model
215 were elastic modulus, yield strength and Poisson's ratio, and the values selected from the
216 literature are shown in Table 3.

217 *FRP Material:* The orthotropic linear elastic material model with the Lamina option
218 was used to model the GFRP wrap used by Harichandran and Baiyasi (2000) in their
219 accelerated corrosion test specimens. Model parameters such as the elastic and shear moduli
220 in all directions and Poisson's ratio were selected based on the mechanical properties
221 provided by the manufacturer and are shown in Table 3.

222 *Concrete Interface*: The interfaces between the concrete/steel tube and
223 concrete/GFRP wrap were assumed to be fully bonded. Full bonding between the surfaces
224 was achieved by using the tie option in ABAQUS.

225 The internal radial pressures that caused the same hoop strains in the steel tube as in
226 the experimental specimens for the water/Bristar ratios of 0.4 and 0.5 were estimated.
227 Figure 3 shows how the strain in the steel tube in the FE model of the calibration specimens

changes with the radial pressure applied to the inside of the center hole. The pressures causing strains of 380 με and 660 με in the steel tube were estimated to be 22 MPa and 25.5 MPa, respectively. These pressures correspond to those that Bristar with water/Bristar ratios of 0.5 and 0.4 applies to the surrounding concrete in the calibration specimens, respectively. These pressures were then applied in the FE model of the calibration specimens with three layers of GFRP wrap and the strains in the wrap were compared with the strain of about 4,000 με measured in the GFRP wrap by Harichandran and Baiyasi (2000). Figure 4 shows the relationship between the internal radial pressure and the GFRP wrap strain in the FE simulations. The strains in the GFRP wrap due to the internal radial pressures of 22 MPa (corresponding to water/Bristar ratio of 0.5) and 25.5 MPa (corresponding to a water/Bristar ratio of 0.4) were 3,800 με and 5,000 με, respectively. As expected, the analytical model was inaccurate and the hoop strains in the GFRP wrap from finite element simulations are lower than those computed by the analytical method. Nevertheless, the FE analysis confirms that the water/Bristar ratio of 0.5 is appropriate to simulate corrosion-induced expansion because the predicted GFRP strain of 3800 με is close to the peak strain of 4,000 με measured by Harichanandran and Baiyasi (2000) for 33% of mass loss in their accelerated corrosion test.

RESULTS AND DISCUSSION

Durability of FRP Panel

Table 4 lists the mechanical properties of the FRP panels before and after freeze-thaw exposure. Note that different sets of specimens were used for the unconditioned modulus and strength tests. It was difficult to control the thickness of panels fabricated using the wet lay-up process and the mechanical properties of the FRP panels are sensitive to specimen

thicknesses. To avoid this sensitivity, the effective stiffness (i.e., modulus × thickness) and ultimate strength per unit width (i.e., ultimate strength × thickness) were used to compare results.

Figure 5 and Table 4 indicate that freeze-thaw conditioning had little effect on the mean effective stiffness of glass panels, while for carbon panels it appears to have increased by 30%, the latter being significant at the 95% level. The decrease of 21% in the mean ultimate strength per unit wideth of glass is significant at the 95% level, but the apparent increase in strength for carbon is not significant at the 95% level (because of the large variation for the unconditioned panels). The decrease of 20% and 28% in the mean ultimate strains of glass and carbon panels, respectively, is significant at the 95% confidence level. It should be noted that many of the failures occurred at the grips and may have been premature. The ultimate strains of the unconditioned and conditioned specimens are significantly lower than the values reported by the manufacturer.

Durability of Confined Concrete

Strength and durability tests were performed on FRP-wrapped round and square cylinders. The primary purpose of the tests was to determine the durability of the FRP tubes under simultaneous corrosion and freeze-thaw cycling, with strength considerations being secondary.

Corrosion expansion: Initially, the expansion due to accelerated corrosion for 190 days causing 33% mass loss was simulated using Bristar. Based on the calibration results reported earlier, the water/Bristar ratio was selected to be 0.5.

Initial strain gauge readings from the FRP wrap were taken prior to pouring Bristar in the center hole of each specimen. Since Bristar is highly porous and water absorption with

274 subsequent freezing and thawing within the hole containing Bristar was undesirable, the ends
275 of the specimens were coated with epoxy prior to the freeze-thaw tests after the Bristar had
276 fully expanded.

277 The average strain in the wraps after adding Bristar varied from 3,100 to 6,000 με for
278 GFRP-wrapped specimens with an average of 4,700 με and 2,400 to 6,800 με for CFRP-
279 wrapped specimens with an average of 4,800 με. Variations in these values occurred because
280 it was not possible to control the pressure exerted by Bristar precisely. However, the average
281 strain values were a little higher than the strain of 4,000 με measured by Harichandran and
282 Baiyasi (2000) in the GFRP wrap due to steel corrosion and 33% mass loss (see Figure 2)
283 and the predictions of 4,500 με and 3,800 με from the analytical and FE models. As shown in
284 Figures 6a and 6b, the round specimens had lower strains (average of 3200 με) that were
285 closer to the FE predictions compared to the square specimens because the Bristar calibration
286 was done using round specimens.

287 *Freeze-Thaw Test:* After corrosion-like expansion of wrapped specimens, they were
288 subjected to freeze-thaw cycles according to the ASTM C666 Procedure B, with freezing in
289 air and thawing in water. Thermocouples mounted at the center of wrapped and unwrapped
290 control specimens were used to measure the internal temperatures during testing. Since the
291 wrapped specimens took longer to reach −17.8°C (end set point for the freeze cycle) and
292 4.4°C (end set point for the thaw cycle) than the unwrapped specimens, the freeze-thaw
293 machine was precisely calibrated before the test. ASTM C666 allows a tolerance of ±1.7°C at
294 the upper and lower set points. By adjusting the sump water temperature during a few trial
295 cycles, it was determined that a sump water temperature of 7.2°C would ensure that all

296 specimens attained temperatures of −17.78±1.7°C at the end of the freeze cycle and
297 4.4±1.7°C at the end of the thaw cycle and thereby the test conformed to ASTM C666.

298 The FRP hoop strains were monitored twice a day during the entire testing period for
299 specimens fitted with strain gauges. Two readings were made each day, one during the freeze
300 phase and the other during the thaw phase. The strains were measured throughout this period.
301 All strain gauges survived the freeze-thaw test. Figures 6a and 6b show the strain in the FRP
302 wraps during the freeze-thaw cycles for GFRP and CFRP, respectively. In general, the strain
303 during the freeze cycle was 100-200 με higher than that during the thaw cycle. This is most
304 likely due to the thermal contraction of the glass wrap during freezing. However, for carbon
305 there was only a slight difference between thaw and freeze readings since its coefficient of
306 thermal expansion is close to zero.

307 *Compression Test:* Figure 7 and Table 5 show results of the compression tests for round
308 and square wrapped specimens without and with freeze-thaw conditioning. All the FRP-
309 wrapped specimens were subjected to corrosion-like expansion simulated with Bristar, all
310 conditioned specimens were subjected to 300 cycles of freeze-thaw cycles, and control
311 specimens were not subjected to freeze-thaw cycles. None of the plain concrete specimens
312 were subjected to corrosion-like expansion simulated by Bristar. The following observations
313 are made:

314 • **Plain round specimens:** Only one of three specimens survived freeze-thaw conditioning
315 for 300 cycles. The two specimens that did not survive had extensive cracking and
316 spalling due to freeze-thaw cycles, which made it impossible to perform compression
317 testing on them. The specimen that survived had approximately the same compression

strength as the control specimens (~35-45 MPa). There was no significant reduction in strength due to freeze-thaw conditioning if the specimen survived.

- **Round glass-wrapped specimens:** In general, conditioning had little effect and the compression strength was approximately the same for control and conditioned specimens. The strength of wrapped specimens (~105-110 MPa) was approximately 2.6 times larger than the strength of unwrapped specimens.
- **Round carbon-wrapped specimens:** Conditioning reduced the compression strength from about 95 MPa to about 80-94 MPa, generally representing about a 15% strength loss. The strength of wrapped specimens (~95 MPa) was approximately 2.3 times larger than the strength of unwrapped specimens.
- **Square glass-wrapped specimens:** Again, conditioning had little effect on the compressive strength (~62-66 MPa). The strength of wrapped specimens was approximately 1.5 times larger than the strength of unwrapped specimens.
- **Square carbon-wrapped specimens:** Conditioning reduced the compression strength slightly from about 58-65 MPa to about 55-63 MPa. The strength of wrapped specimens (~60 MPa) was approximately 1.4 times larger than the strength of unwrapped specimens.

The wrapped square prisms had lower compressive strength compared to the wrapped round cylinders, even though the cross sectional area of the prisms was higher than that of the cylinders. This was due to the reduced confinement provided by the wraps for square cross sections and stress concentrations that develop at the corners. For square prisms, glass and carbon wraps increased the strength by about the same amount. Wrapped square prisms always failed by rupture of the wrap at a corner. A reduction in compression strength of

approximately 30-40% was observed between the round cylinders and the square prisms. The wrapped square prisms also demonstrated a sudden loss of strength after the peak stress was reached. However, the wraps were undamaged during this loss of strength. The loss of strength was most likely due to the failure of the ineffectively confined regions of concrete. These regions do not experience capacity enhancement due to poor confinement.

Table 5 shows the mean ultimate compression strengths and 95% confidence margins for each category of specimens. The cross sectional area lost by the cavity containing Bristar was deducted when calculating the strengths. At the 95% confidence level, means of the compressive strength of specimens subjected to freeze-thaw cycles are not significantly different from those of control specimens. Similarly, the freeze-thaw cycles have no statistically significant effect on the compressive strength of square prisms. The reduction in mean compressive strength observed for carbon-wrapped specimens after freeze-thaw conditioning is not statistically significant for the sample size used in this study.

SUMMARY AND CONCLUSIONS

Strength and durability tests were carried out on round cylinders and square prisms made of concrete and wrapped with glass and carbon FRP. An expanding cement known as Bristar was used in the wrapped specimens to investigate the durability of glass and carbon wraps under sustained expansion load and subjected to freeze-thaw cycling. The sustained expansion load simulated the load generated in wrapped columns by corrosion products. Chloride was impregnated into the cylinders during casting in order to simulate concrete exposed to salt. The compression strength of plain control cylinders as well as wrapped test

specimens after 300 cycles of freeze-thaw conditioning was measured. A total of 60 specimens were used in the freeze-thaw test.

The means of the compressive strength of freeze thaw specimens were not significantly different from those of control specimens at the 95% confidence level. This was true both for carbon and glass wraps, and for specimens with round and square cross sections. The results indicate that the wraps did not sustain significant damage due to freeze-thaw cycling under sustained load.

The wrapped square prisms had lower compressive strengths compared to the wrapped round cylinders, even though the cross sectional area of the square prisms was higher than that of the round cylinders. This was due to the reduced confinement provided by the wraps for square cross sections and stress concentrations that develop at the corners. Wrapped square prisms always failed by rupture of the wrap at a corner. A reduction in the failure strength of approximately 30-40% was observed for the square specimens compared to the round specimens.

The compression strength of wrapped specimens was 1.4 to 2.6 times larger than that of unwrapped specimens for square and round cross sections, respectively.

ACKNOWLEDGEMENTS

This research was sponsored by the Michigan Department of Transportation.

REFERENCES

Almusallam, T. H., Al-Salloume, Y. A., and Alsayed, S. H. (2000). "Durability of concrete cylinders wrapped with GFRP sheets at different environmental conditioning." *Seventh*

386 *Annual International Conference on Composites Engineering*, Denver, Colorado, July 2-
387 8, 27-28.
388
389 Arya, C., and Sa'id-Shawqi, Q. (1996). "Factors influencing electrochemical removal of
390 chloride from concrete." *Cement and Concrete Research*, 26(6), 851-860.
391
392
393 Chajes, M.J., Mertz, D.R., and Thomson, T.A. (1994). "Durability of composite material
394 reinforcement." *Proceedings*, *Third Materials Engineering Conference*, ASCE, San
395 Diego, California.
396
397 Chin, J. W., Nguyen, T., and Aouadi, K. (1997). "Effects of environmental exposure on
398 fiber-reinforced plastic (FRP) materials used in construction." *Journal of Composites*
399 *Technology and Research*, 19(4), 205-213,
400
401 Colombi, P., Fava. G. and Poggi, C., (2010). "Bond strength of CFRP-concrete elements
402 under freeze-thaw cycles." *Composite Structures*, 92(4), 973-983.
403
404 Du, Y. G., Chan, A. H. C., and Clark, L.A (2006). "Finite element analysis of the effects of
405 radial expansion of corroded reinforcement." *Computers and Structures*, 84(13-14), 917-
406 929.
407
408 El-Zefzafy, H., Mohamed, H. M., and Masmoudi, R. (2011). "Freeze-thaw effects on the
409 behavior of concrete-filled FRP tube columns." *Proceedings,* Annual Conference of the
410 Canadian Society for Civil Engineering, 2, 1563-1572.
411
412 Gomez, J., and Casto, B. (1996). "Freeze-thaw durability of composite materials."
413 *Proceedings,* 1st International Conference on Composites in Infrastructure (ICCI),
414 Tucson, AZ, 947–955.
415
416 Green, M. F., Bisby, L. A., Fam, A. Z., and Kodur, V. K. (2006). "FRP confined concrete
417 columns: behaviour under extreme conditions." *Cement and Concrete Composites*,
418 28(10), 928-937.
419
420 Harichandran, R. S., and Baiyasi, M. I. (2000). "Repair of corrosion-damaged columns using
421 FRP wraps." *Report No. RC-1386*, Michigan Department of Transportation, Lansing,
422 Michigan.
423
424 Karbhari, V. M. and Zhao, L., (1998). "Issues related to composite plating and environmental
425 exposure effects on composite-concrete interface in external strengthening." *Composite*
426 *Structures,* 40(3/4), 293–304.
427
428 Li, Y., and Karbhari, V. M. (2003). "Durability characterization of T700 based composites
429 for use in civil infrastructure." Proceedings, 44th International SAMPE Symposium and
430 Exhibition, Vol. II, 1540-1552.

Mehta, P., and Monteiro, J. (1993). *Concrete, structure, properties, and materials*. Second Edition, Prentice-Hall, Englewood Cliffs, 160-164.

Nardone, F., Di Ludovico, M., De Caso Y., Basalo, F. J., Prota, A., and Nanni, A. (2012). "Tensile behavior of epoxy based FRP composites under extreme service conditions." *Composites Part B: Engineering*, 43(3), 1468-1474.

Rivera, J., and Karbhari, V. (1999). "Effects of extended freeze-thaw exposure on composite wrapped concrete cylinders." *Proceedings*, 44th SAMPE Symposium, Long Beach, California, May 23-27.

Shi, J., Zhu, H., Wu, Z., Seracino, R., and Wu, G. (2013). "Bond behavior between basalt fiber–reinforced polymer sheet and concrete substrate under the coupled effects of freeze-thaw cycling and sustained load." *Composites in Construction*, 17(4), 530-542.

Silva, M. A. G, and Biscaia, H. (2008). "Degradation of bond between FRP and RC beams." *Composite Structures*, 85(2), 164-174.

Soudki, K. A. (1997). "Freeze-thaw response of CFRP wrapped concrete." *Concrete International*, 19(8), 64-67.

Steckel, G. L., Hawkins, G. F., and Bauer, J. L. (1998). "Environmental durability of composites for seismic retrofit of bridge columns." *2nd International Conference on Fiber Composites in Infrastructure ICCI* ,Vol.2, Tucson, 460–475.

Toutanji, H., and Balaguru, P. (1998). "Durability characteristics of concrete columns wrapped with FRP tow sheets." *Journal of Materials in Civil Engineering*, 10(1), 52-57.

Toutanji, H., and El-Korchi, T. (1999). "Tensile durability of cement-based FRP composite wrapped specimens." *Journal of Composites for Construction*, ASCE, 3(1), 38-45.

Yu, T., Teng, J. G., Wong, Y. L., and Dong, S. L. (2010). "Finite element modeling of confined concrete-I: Drucker-Prager type plasticity model." *Engineering Structures*, 32(3), 665-679.

Yun, Y., and Wu, Y. F. (2011). "Durability of CFRP-concrete joints under freeze-thaw cycling." *Cold Reg. Sci. Technol.*, 65(3), 401–412.

Table 1: Freeze-Thaw Laboratory Testing Matrix

Specimen Type	Conditioning	No. of Specimens		
		Unwrapped	GFRP	CFRP
Round	None	3	3	3
Square			3	3
Round	300 cycles of freeze-thaw	3	3	3
Square			3	3

Table 2: Analytical Estimate of Maximum Confining Pressure and GFRP Strain

Water/Bristar Ratio	Measured Strain (με)	Confining Pressure (MPa)	Strain in GFRP (με)
0.5	380	4.76	4500
0.4	660	8.27	7800

485 **Table 3:** Parameters used in FE Analysis
486
487
488
489
490
491
492
493
494
495

Materials	**Elastic Modulus (GPa)**	**Strength (MPa)**	**Thickness (mm)**	**Poisson's Ratio**
Concrete	28.8	(Compressive) 37.7	NA	0.16
Steel	200.0	410.0	4.77	0.3
GFRP	(Fiber direction) 27.6	NA	1.00	0.29

496 **Table 4:** Mechanical Properties of FRP Panels Before and After Freeze-Thaw Exposure

Wrap Type	Thickness (mm)	Modulus (MPa)	Effective Stiffness (N/mm)	Ultimate Strength per Unit Width (N/mm)	Ultimate Strain
		No Exposure			
GFRP	1.227	22,011	27,000	536	0.02
CFRP	0.625	53,061	33,150	415	0.015
		300 Freeze-Thaw Cycles			
GFRP	1.092	23,805	26,000	424	0.016
CFRP	0.508	79,012	40,138	448	0.01

497
498

Table 5: Compression Test Summary Data

Specimens Type			Ultimate Compressive Strength (kPa)		
Wrap	**Shape**	**Condition**	**Average**	**Standard Deviation**	**95% Conf. Margin**
No Wrap	Round	Control	41,074	2,531	±2,656
		F/T	42,875	NA	NA
GFRP	Square	Control	63,601	1,907	±2,002
		F/T	63,761	1,208	±3,002
	Round	Control	109,911	3,856	±6,136
		F/T	108,370	1,727	±4,291
CFRP	Square	Control	91,924	2,652	±2,783
		F/T	59,384	3,149	±7,822
	Round	Control	92,558	3,612	±3,791
		F/T	84,714	8,440	±20,967

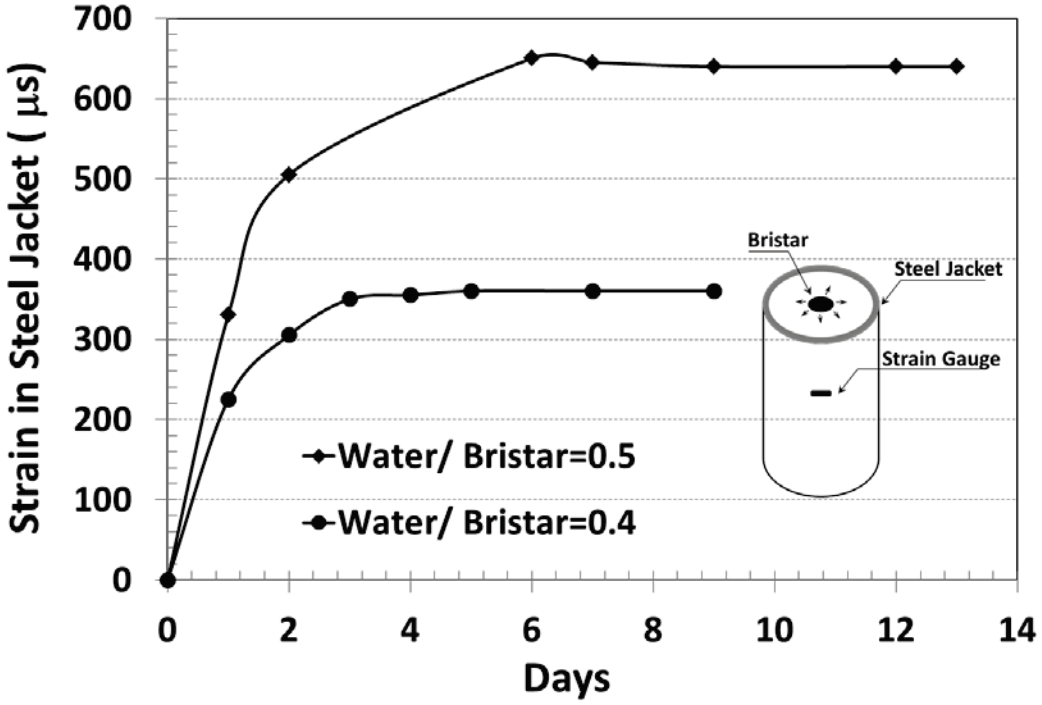

Figure 1: Strain in steel tube for different water to Bristar ratios

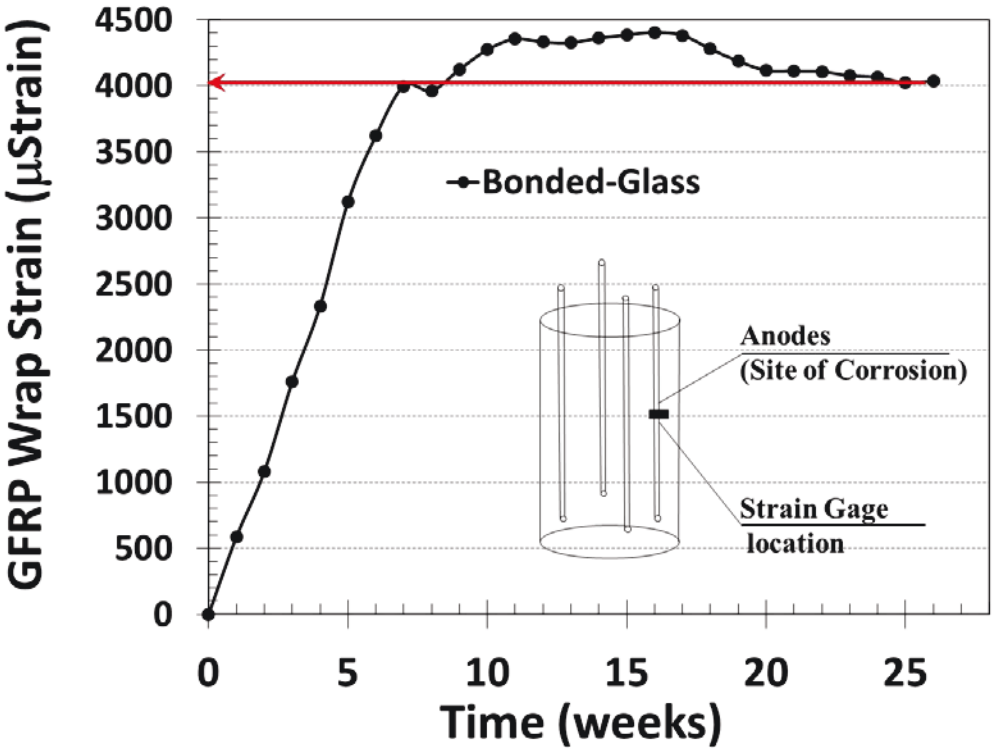

Figure 2: Strain developed in GFRP wrap in accelerated corrosion test (Harichandran and Baiyasi 2000)

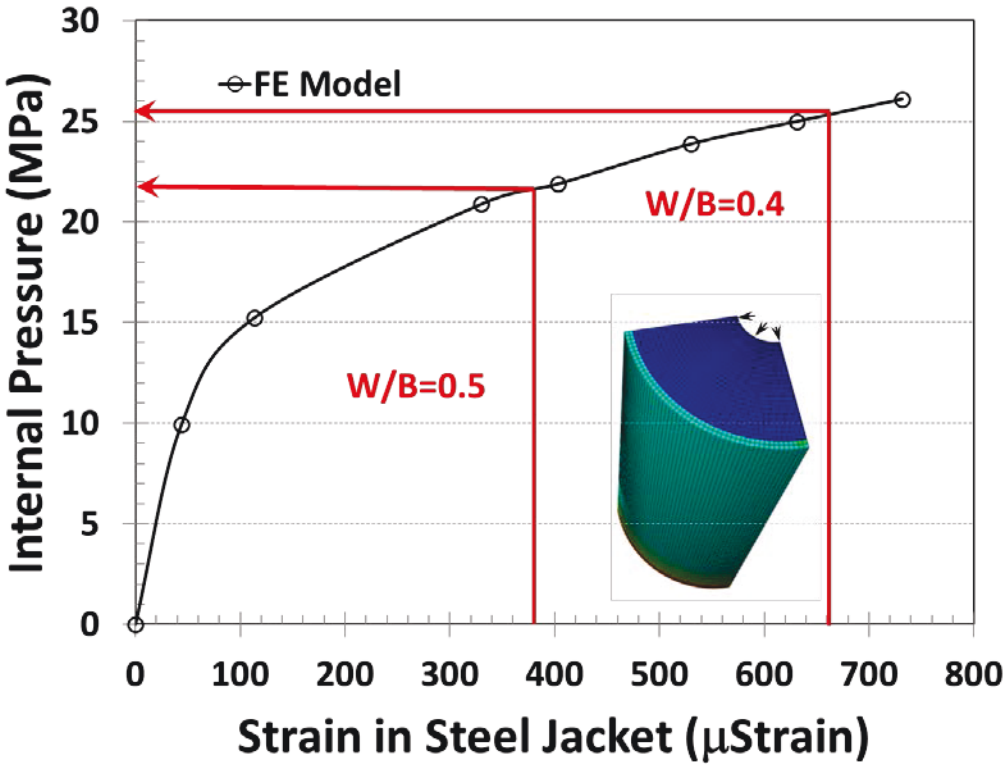

Figure 3: Strain developed in steel tube in FE model of calibration specimens

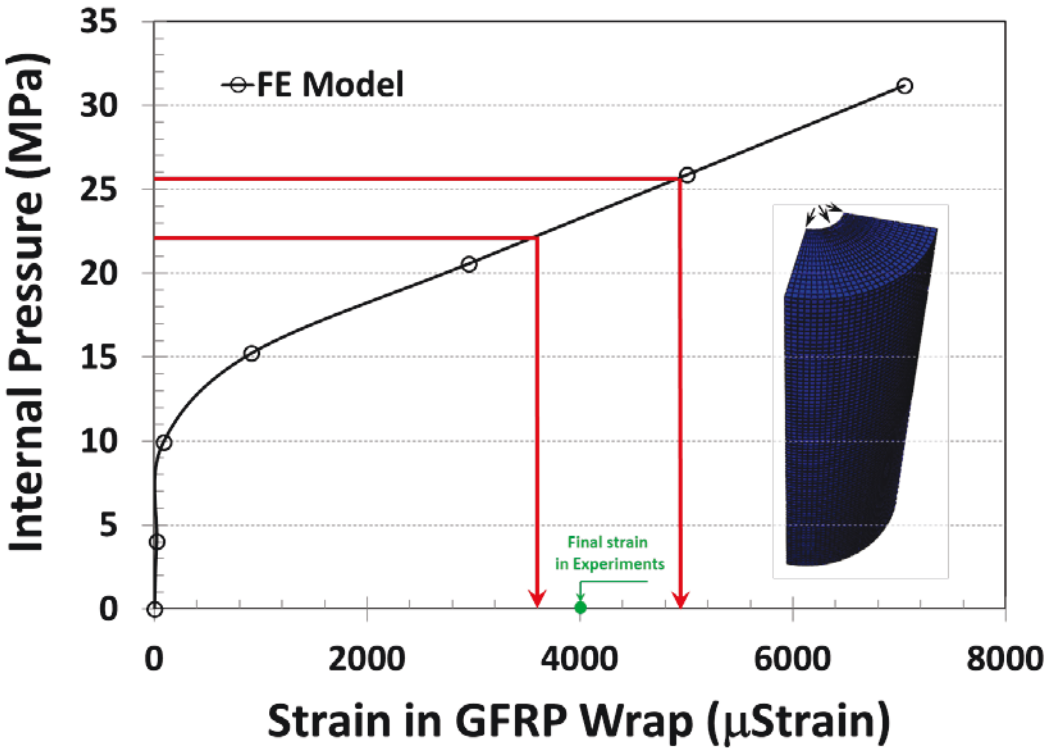

Figure 4: Strain developed in GFRP wrap in FE model of test specimens

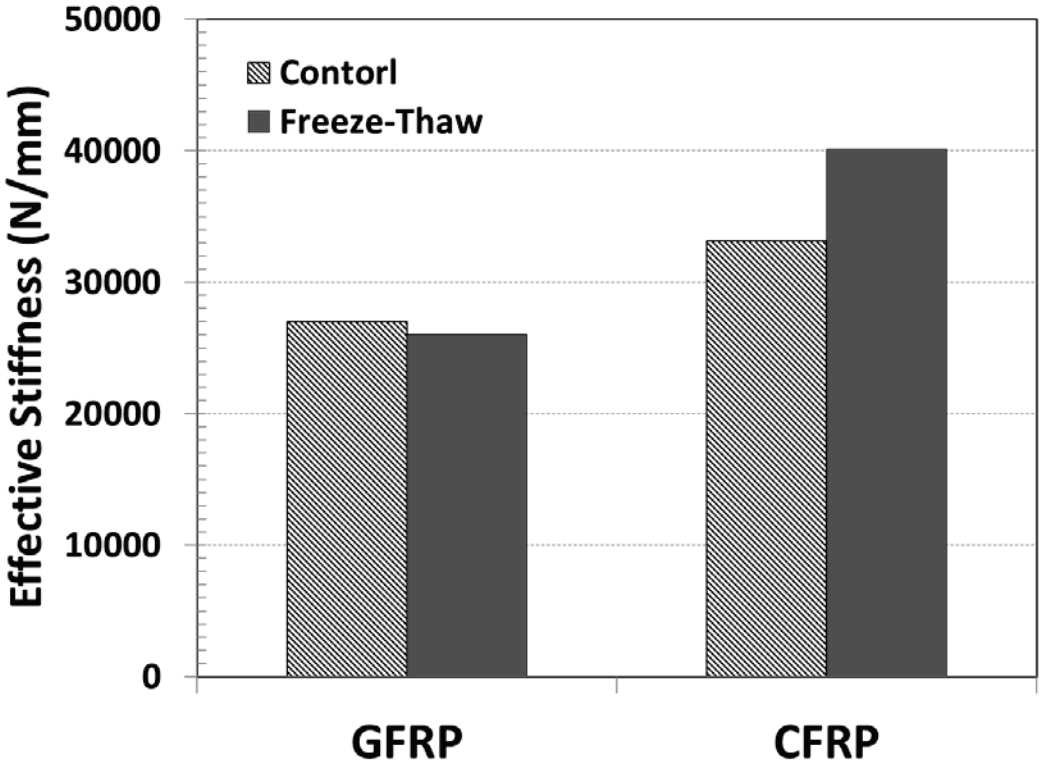

Figure 5: Effective stiffness of FRP panels after 300 freeze-thaw cycles

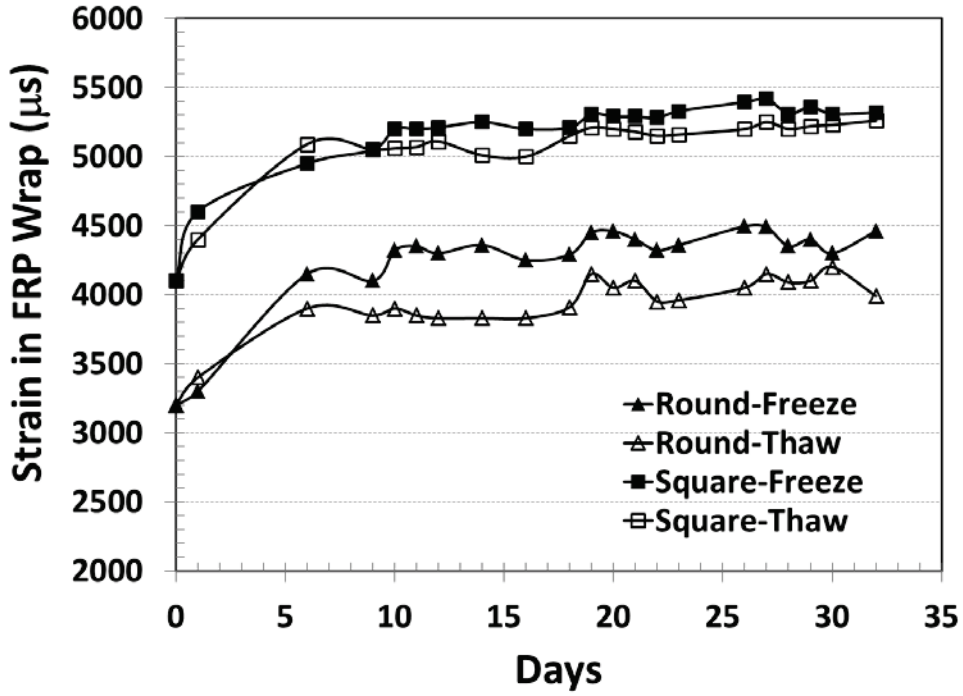

(a)

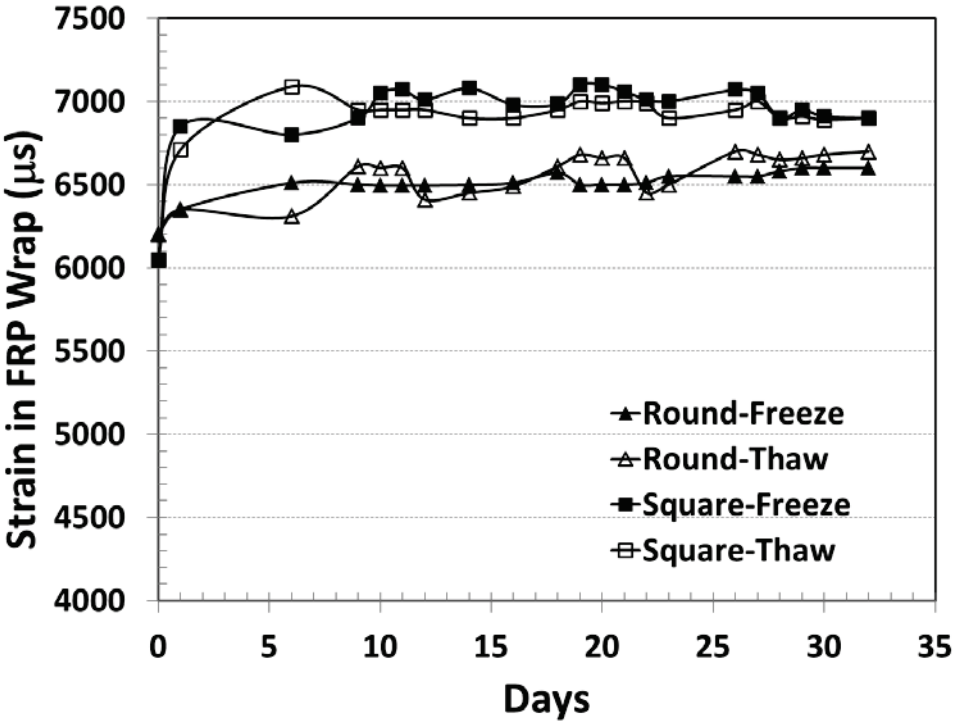

(b)

Figure 6: Strain in FRP wrap during freeze-thaw cycles (a) glass, (b) carbon

626

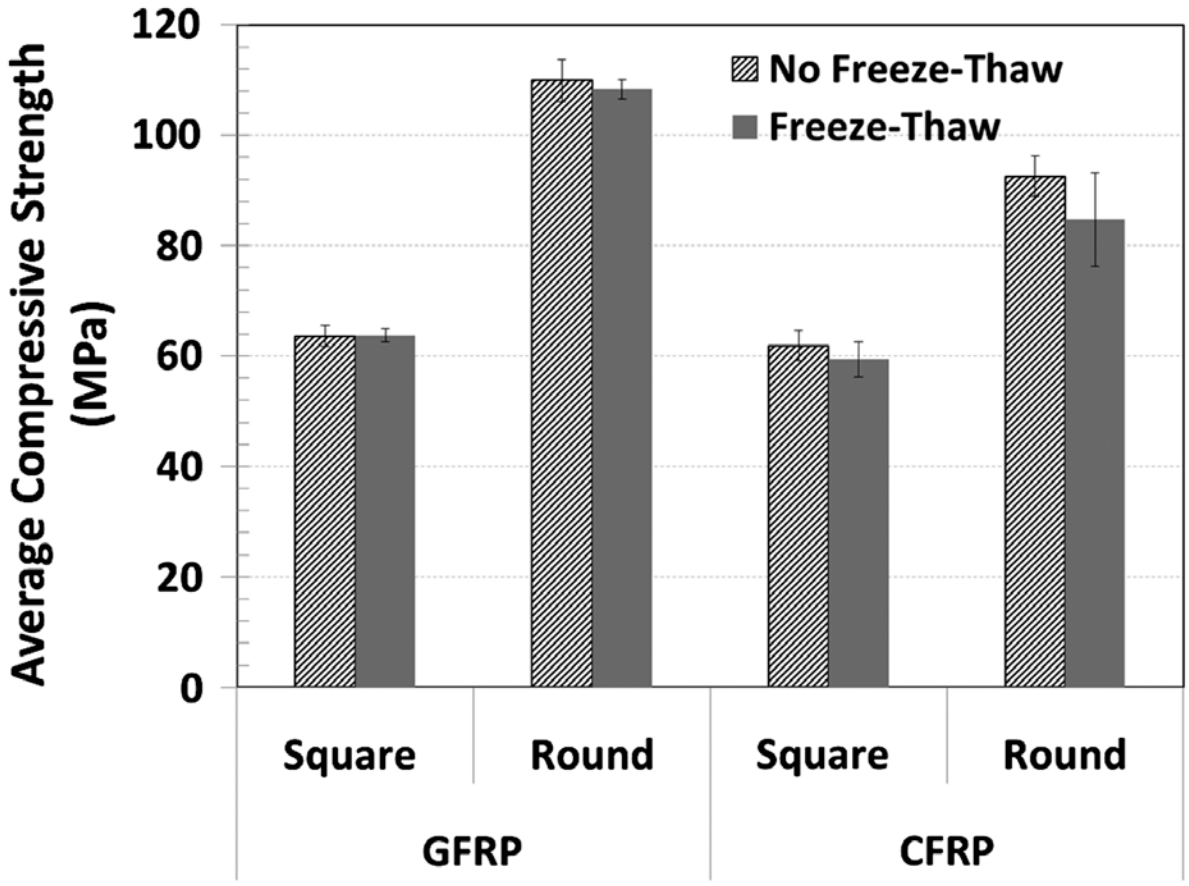

627
628
629
630 **Figure 7:** Results of the compression tests for round and square wrapped specimens
631